Sixth International Symposium on Turbulence and Shear Flow Phenomena
Seoul, Korea, 22-24 June 2009

ASBM-BSL: AN EASY ACCESS TO THE STRUCTURE BASED MODEL TECHNOLOGY

Bertrand Aupoix
Aerodynamics and Energetics Department, ONERA
BP 74025 - 2, Avenue E. Belin - 31055 Toulouse Cedex 4, France
Bertrand.Aupoix@onera.fr

Stavros C. Kassinos & Carlos A. Langer
Computational Sciences Laboratory – UCY-CompSci, Department of Mechanical & Manufacturing Engineering
University of Cyprus, 75 Kallipoleos, Nicosia 1678, Cyprus
kassinos@ucy.ac.cy, langer@ucy.ac.cy

ABSTRACT

The Algebraic Structure Base Model (ASBM), which gives a more complete description of turbulence than classical models, has been coupled with the $k-\omega$ BSL transport equations to allow an easy use of this model. As the ASBM model requires correct estimates of the turbulent kinetic energy and dissipation rate, a correction of the relation between ω and the dissipation rate in the wall region is proposed. First tests on simple flows show encouraging results.

INTRODUCTION

Present industrial design heavily relies upon CFD, using mainly eddy viscosity models, the two most popular ones being the Spalart-Allmaras (1994) one equation model and the Menter SST $k-\omega$ model (1992), because of their ability to predict separation. However, they are known to fail to capture many flow issues, first of all because of the eddy viscosity assumption.

Two routes are generally considered to get rid of the eddy viscosity assumption:

• The use of transport equations for the Reynolds stress tensor (DRSM models) allows one to circumvent most of the failures of the eddy viscosity assumption, by accounting for turbulence memory effects and most of the rotation and curvature effects. Although the FLOMANIA project (Haase et al., 2006) led to robust implementation of such models in several CFD codes, their everyday use is still an issue.

• Explicit Algebraic Reynolds Stress Models (EARSM) only require two transport equations and replace the eddy viscosity assumption by an equilibrium assumption for the anisotropy tensor. They so inherit many properties of the underlying Reynolds stress model. However, the extension of these models in regions where the equilibrium assumption does not hold has long been an issue.

A third modelling route was proposed by Reynolds et al. (2000) and Kassinos et al. (2000, 2001) to circumvent most of the failures of DRSM models. While DRSM models assume that all the information about turbulence is in the turbulence length and velocity scales and in the anisotropy tensor, they pointed out the importance of the dimensionality of turbulence. This led them to Structure Based Models (SBM), which are able to better represent rapid distortion, rotation effects and many subtle non-equilibrium effects than current DRSM models. But these models use extra transport equations, compared to DRSM models and are thus less prone to a prompt industrial use.

A simplified version, using the SBM approach to directly represent the anisotropy and dimensionality tensors was derived (Kassinos et al., 1994; Langer and Reynolds, 2003). It only requires two transport equations for turbulence velocity and length scales, and brings some similarities with EARSM models. This approach is very powerful as it allows to sensitize the length scale equation to the dimensionality of turbulence. But the length scale equation (Reynolds et al., 2002) is unusual and may require some specific changes to be implemented in a commercial code.

Therefore, an even more simplified version, coupling the Algebraic Structure Based Model (ASBM) with a more standard set of length scale equations, has been developed, to give an easy access to the ASBM technology.

ASBM MODELLING

Structure Based Models, and especially ASBM models, can be envisioned in two complementary ways.

A first way is the use of turbulence structure tensors to characterize the turbulent motion. While DRSM models only deal with the anisotropy tensor, other tensors can be derived from the turbulent stream function vector, the curl of which is the turbulent velocity field. The dimensionality tensor characterizes the changes of the turbulence structure along the various directions; the circulicity tensor characterizes the vorticity field associated with the energy bearing structures, the inhomogeneity tensor the degree of inhomogeneity of the turbulent field. These three tensors and the Reynolds stress tensor are related and, in SBM complete models, transport equations are solved for these tensors to fully describe the turbulent field.

A second way is to consider that turbulence can be mimicked with a combination of simplified turbulent structures, i.e. as an ensemble of hypothetical 2D eddies the direction of independence of which is aligned with the eddy-axis. These eddies differ by their componentality and dimensionality and are:

• Jetal motions: 2D-1C fields where the motion is only along the eddy axis,

• Vortical motions: 2D-2C fields where the motion is around the eddy axis,

• Helical eddies: superpositions of the above two motions

A last important notion is the flattening of the eddies, which is related to the degree of asymmetry of the turbulent kinetic energy distribution around the hypothetical eddies.

A complete turbulent field is envisioned as a large ensemble of these eddies, with varying characters and orientations. Averaging over the ensemble produces statistical quantities representative of the field. Decomposing the fluctuating velocity in components aligned and normal to the eddy-axis direction, taking the product $u_i'u_j'$, and then averaging, results in the algebraic constitutive relation for the normalized Reynolds stress tensor (related to statistics of the ensemble)

$$\begin{aligned} r_{ij} = \frac{\overline{u_i'u_j'}}{2k} = \tfrac{1}{2}(1-\phi)(\delta_{ij}-a_{ij}) + \phi a_{ij} \\ +(1-\phi)\chi\left[\tfrac{1}{2}(1-a_{nm}b_{nm})\delta_{ij} - \tfrac{1}{2}(1+a_{nm}b_{nm})a_{ij}\right. \\ \left. -b_{ij} + a_{in}b_{nj} + a_{jn}b_{ni}\right] \\ -\gamma\frac{\Omega_k}{\Omega}(\epsilon_{ipr}a_{pj}+\epsilon_{jpr}a_{pi})\left\{\tfrac{1}{2}\left[1-\chi(1-a_{nm}b_{nm})\right]\delta_{kr}\right. \\ \left. +\chi(b_{kr}-a_{kn}b_{nr})\right\} \end{aligned} \tag{1}$$

where a_{ij}, the eddy-axis tensor, represents the energy-weighted average direction cosine of the eddy-axis vector. Eddies, like material lines, tend to align with the direction of positive mean strain rate, and are rotated kinematically by the mean rotation rate. To ensure the algebraic model for the eddy-axis tensor is realizable, it is computed via a two-step procedure. Initially a strained eddy axis, a_{ij}^s, is evaluated based upon the mean strain rate tensor, S_{ij}.

$$a_{ij}^s = \frac{\delta_{ij}}{3} + \tau\frac{S_{ik}a_{kj}^s + S_{jk}a_{ki}^s - \frac{2}{3}|Sa^s|\delta_{ij}}{a_0 + 2\sqrt{a_1^2 + \tau^2 S_{kp}S_{kq}a_{pq}^s}}, \tag{2}$$

where τ is a turbulent time scale, $|Sa^s| = S_{pq}a_{qp}^s$, and $\{a_0,\ a_1\}$ are "slow" parameters. Next a rotation operation is applied on a_{ij}^s, so that the final (strained, then rotated) eddy-axis tensor, a_{ij}, is obtained as

$$a_{ij} = H_{ik}H_{jm}a_{ij}^s. \tag{3}$$

The rotation operator H_{ij} is modeled as

$$H_{ij} = \delta_{ij} + h_1\frac{\Omega_{ij}}{\sqrt{|\Omega^2|}} + h_2\frac{\Omega_{ik}\Omega_{kj}}{|\Omega^2|}, \tag{4}$$

which satisfies the orthonormal conditions $H_{ik}H_{jk} = \delta_{ij}$ for $h_1 = \sqrt{2h_2 - h_2^2/2}$. h_2 is chosen to satisfy theoretical rapid distortion limits for combined homogeneous plane strain and rotation.

$$h_2 = \begin{cases} 2 - 2\sqrt{(1+\sqrt{1-r}\,)/2} & \text{if } r \le 1 \\ 2 - 2\sqrt{(1-\sqrt{1-1/r}\,)/2} & \text{if } r \ge 1 \end{cases},$$

where $r = (a_{pq}\Omega_{qr}S_{rp})/(S_{kn}S_{nm}a_{mk})$.

b_{ij}, the eddy-flattening tensor, is an ensemble average of the direction cosines of the eddy-flattening vector. The flattening direction is found to be dependent on the vorticity vector, and the model for b_{ij} takes the simple form (fixed frame)

$$b_{ij} = \frac{\Omega_i\Omega_j}{|\Omega^2|}. \tag{5}$$

ϕ, the jetal parameter, is representative of the amount of energy in the jetal mode of motion. $(1-\phi)$ is representative of the amount of energy in the vortical mode. In irrotational flows $\phi = 0$, and of course $0 \le \phi \le 1$. Mathematically, it represents the average (over all eddies) of the dot product between the eddy-axis vector and the velocity vector. In simple shear flows (this study), it reads

$$\begin{aligned} \phi &= 1 \times f_{\text{slow}}(a^2) \\ f_{\text{slow}}(a^2) &= 0.35 f_{\text{iso}}^{2.5}(a^2) + (1-0.35) f_{\text{iso}}^{0.5}(a^2) \\ f_{\text{iso}}(a^2) &= (3/2)(a^2 - 1/3) \end{aligned} \tag{6}$$

γ, the helical parameter, is representative of the correlation between the jetal and the vortical modes. In the general case,

$$\gamma = \beta\sqrt{\frac{2\phi(1-\phi)}{1+\chi}}, \tag{7}$$

and for simple shear flows $\beta = 1$.

χ is the flattening parameter, a representative of the average magnitude of the lack of symmetry in the energy distribution around the eddies. In simple shear flows

$$\chi = 0.2 \times f_{\text{slow}}(a^2). \tag{8}$$

The model is moreover sensitized to the wall blocking with the help of an elliptic relaxation equation for a blocking parameter Φ, from which a partial projection of the eddy axis tensor towards the wall is deduced

$$\begin{aligned} a_{ij} &= P_{ik}a_{kl}^h P_{lj}, \qquad P_{ik} = \frac{1}{D_a}(\delta_{ik} - B_{ik}), \\ D_a^2 &= 1 - (2 - B_{kk})a_{mn}^h B_{nm}, \end{aligned} \tag{9}$$

where P_{ik} is the partial-projection operator, and D_a^2 is such that the trace of a_{ij} remains unity (note the superscript "h" is used to indicate the unblocked tensor). The blockage tensor B_{ij} gives the strength and the direction of the projection. If the wall-normal direction is x_2, then $B_{22} = \Phi$ is the sole non-zero component, and varies between 0 (no blocking) far enough from the wall, to 1 (full blocking) at the wall.

The blocking parameter, Φ, is computed by an elliptic relaxation equation

$$L^2\frac{\partial^2\Phi}{\partial x_l^2} = \Phi, \quad L = C_L \max\left(\frac{k^{3/2}}{\varepsilon}, C_\nu\sqrt[4]{\frac{\nu^3}{\varepsilon}}\right) \tag{10}$$

with $\Phi = 1$ at solid boundaries, and $\dfrac{\partial\Phi}{\partial x_n} = 0$ at open boundaries, where x_n is the direction normal to the boundary. Values of the constants are $C_L = 0.17$, $C_\nu = 80$.

To retrieve the proper near-wall asymptotics for the Reynolds stress tensor, the blocking parameter Φ is also used for blending of ϕ and γ with their wall values; 1 and 0 respectively,

$$\phi = 1 + (\phi^h - 1)(1-\Phi)^2, \tag{11}$$

$$\gamma = \gamma^h(1-\Phi). \tag{12}$$

It must be pointed out that the so obtained Reynolds stress tensor is fully realizable. Model details can be found in Reynolds et al. (2000) and Langer and Reynolds (2003).

COUPLING WITH A k - ω MODEL

Among two-equation models, the $k-\omega$ model is known to give fair predictions of pressure gradient effects. However, as the Wilcox (1988) model is sensitive to free stream values, Menter's BSL model (1994) has been preferred. Coupling the above ASBM representation of the Reynolds stress tensor with the BSL model however requires some changes.

To take advantage of the fair representation of the Reynolds stress tensor provided by the ASBM model, the turbulent kinetic energy production must be computed with the ASBM model as $P_k = -\overline{u_i'u_j'}\frac{\partial U_i}{\partial x_j}$, where the ASBM model provides the expression for the Reynolds stress tensor. The source term in the ω equation deserves more attention. In the original ω equation, thanks to the eddy viscosity definition, it can be expressed, as pointed out by Menter (1994), either as $P_\omega = \gamma P_k \dfrac{\omega}{k}$ or as $P_\omega = 2\gamma S_{ij} S_{ij}$ where S_{ij} is the mean rate of strain. The two expressions differ when the ASBM model is used to express the Reynolds stress tensor. As pointed out by Menter, the second form should be favoured as it states that the turbulence time scale ω^{-1} tends to adjust to the mean flow time scale $\left(\sqrt{2S_{ij}S_{ij}}\right)^{-1}$.

An important point is that the ASBM model has been designed to represent real near wall turbulence while the basic $k-\omega$ model yields turbulent kinetic energy profiles which are more similar to $\overline{v'^2}$ profiles in the wall region and do not exhibit a near-wall peak. Wilcox later proposed to add three wall functions to retrieve the correct wall behaviour. When using the ASBM model, only the dissipation rate is altered as

$$\varepsilon = \beta f_w \omega k \tag{13}$$

A first damping function was adapted from Peng et al. (1997). Results are presented in Aupoix et al. (2009).

A way to optimize the damping function f_w has since been devised. Assuming infinite Reynolds number, the equations in the wall region reduce to a parallel flow, i.e. a one-dimensional problem. Using wall variables, i.e. making all quantities non-dimensional with the wall friction and the viscosity, the model equations reduce to

$$1 = \frac{\partial u^+}{\partial y^+} - \overline{u'v'}^+ \tag{14}$$

$$-\overline{u'v'}^+ = k^+ \mathcal{F}\left(\frac{\partial u^+}{\partial y^+}, k^+, \varepsilon^+\right) \tag{15}$$

$$0 = P_k^+ - \varepsilon^+ + \frac{\partial}{\partial y^+}\left[\left(1 + \sigma \nu_t^+\right)\frac{\partial k^+}{\partial y^+}\right] \tag{16}$$

$$0 = P_\omega^+ - \beta^* \omega^{+2} + \frac{\partial}{\partial y^+}\left[\left(1 + \sigma \nu_t^+\right)\frac{\partial \omega^+}{\partial y^+}\right] \tag{17}$$

$$\nu_t^+ = \frac{k^+}{\omega^+} \tag{18}$$

Equation (14) is the mean flow momentum equation, neglecting advection and pressure gradient effects. As the mean velocity profile is nearly universal, using e.g. Reichardt's $u^+(y^+)$ distribution yields $\frac{\partial u^+}{\partial y^+}$ and hence $\overline{u'v'}^+$. Reichardt's law was slightly modified in the linear region to avoid negative turbulent shear stress $-\overline{u'v'}^+$.

Equation (15) is just a rewriting of the ASBM model (1) in which $\mathcal{F}$ is non-local because of the elliptical relaxation. Provided the ε^+ profile is known, it gives the k^+ profile.

Equation (17) is the BSL (or $k-\omega$ as they are equivalent in the wall region) ω transport equation. From the above determined k^+ profile, it provides the ω^+ profile. It must be noticed that iterations are needed as ω^+ also appears in the definition of the eddy viscosity (18).

At last, the turbulent kinetic energy equation (16) allows to compute the dissipation profile. The complete near wall solution can so be determined, using an iterative process on the dissipation profile and solving all equations from the wall to far in the logarithmic law. As equation (16) requires the derivatives of k^+, some numerical noise issues have to be circumvented. The wall damping function f_w is finally deduced from the turbulent profiles, using equation (13).

Unfortunately, the so-obtained solutions are not fully satisfactory. The turbulent kinetic energy profile is realistic, but the dissipation profile exhibits unexpected oscillations in the buffer region. Playing with the coefficient in the elliptic damping and with the expression for the source term in the ω equation cannot suppress this oscillation which is

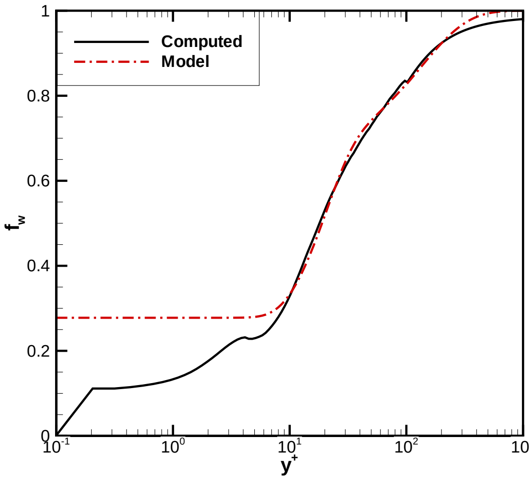

Figure 1: Determination of the wall function

due to an inconsistency between the imposed velocity gradient (and hence turbulent shear stress) distribution and the form of the diffusion term in the turbulent kinetic energy equation (16).

Therefore, a simpler solution was looked for. The turbulent kinetic energy equation (16) was no longer considered and the dissipation profile was imposed. This is justified by the analysis of several DNS (Spalart, 1988; Skote, 1998, Hoyas and Jimenez, 2006) which shows that the near wall dissipation profile is nearly universal for moderate pressure gradient flows. The convergence only deals with the turbulent kinetic energy and specific dissipation profiles.

As pointed out by Wilcox (1993) and Peng et al. (1997), f_w must tend to $\dfrac{5}{18}$ at the wall in order to have $k \propto y^2$ in the wall region and a finite wall value for the dissipation. This has drastic consequences as this limiting behaviour has to be forced in a significant part of the buffer region where the two expressions of P_ω significantly differ. Unfortunately, the choice of $P_\omega = 2\gamma S_{ij} S_{ij}$ leads to a too extended blocking of the f_w function in the buffer layer and thus an overestimation of the dissipation and an underestimation of the turbulent kinetic energy. Better results are achieved using $P_\omega = \gamma P_k \dfrac{\omega}{k}$.

The so-determined f_w function was finally represented as

$$f_w = 1. - \frac{13}{18}\exp\left[-\left(0.6 + \frac{R_t}{50}\right)\left(1. - \exp\left[-\left(\frac{R_t}{10}\right)^2\right]\right)\right]$$

$$R_t = \frac{k}{\nu\omega} \tag{19}$$

This analytical model is compared to the function given by the resolution of the equations in figure 1. Of course, the biggest differences are due to the enforcement of the near-wall behaviour. It must be pointed out that this function plays a rôle rather far from the wall, up to a reduced wall distance y^+ larger than 300 (this value is not linked to the integration domain, which at least extended up to $y^+ = 3000$).

VALIDATION RESULTS

All validation tests were performed with simple one-dimensional codes for self-similar flows or with a boundary

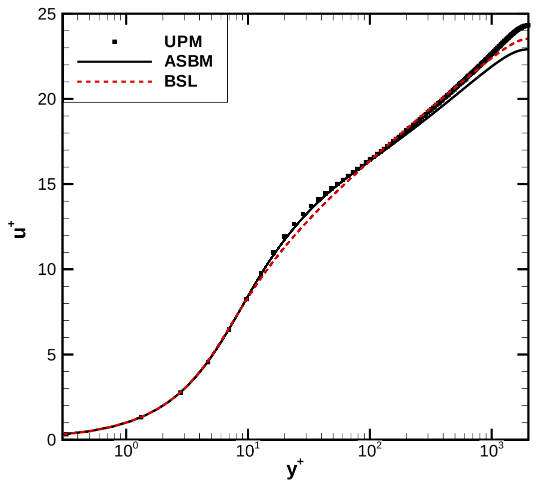

Figure 2: Channel flow $R_\tau = 2000$ – Mean velocity predictions

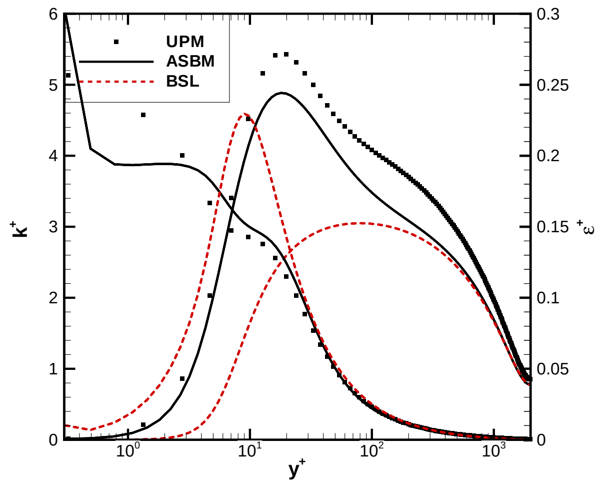

Figure 3: Channel flow $R_\tau = 2000$ – Turbulent kinetic energy and dissipation rate predictions

layer code with adaptive grid so that grid convergence is achieved.

Channel flows

Channel flows are first addressed. Predictions of the pressure drop versus Reynolds number remain within ±4% over the investigated range, i.e. up to a Reynolds number based upon the mass flow velocity $Re = \frac{2\overline{u}h}{\nu} = 6\,10^5$, where h is the channel half height. The accuracy is better than that of the BSL model and other tested models (mixing length, $k-\varepsilon$).

Predicted profiles are compared with DNS data at various Reynolds numbers, provided by Madrid Polytechnic University (Hoyas, 2006). For the sake of clarity, only the present ASBM model and the standard BSL model are presented, and only for the largest Reynolds number $R_\tau = \frac{hu_\tau}{\nu} = 2000$. All figures use wall scaling.

The mean velocity profiles are presented in Figure 2. The near wall treatment of the ASBM model is fair as the buffer region is better predicted than with the standard BSL model. Both models depart from the DNS in the wake region, which is consistent with the error on the pressure drop for this Reynolds number.

Figure 3 points out that the model rather nicely reproduces the turbulent kinetic energy profile, but underestimates it as it cannot capture the inactive motions, as will be discussed later. On the contrary, the turbulent kinetic energy profile predicted by the BSL model is unrealistic as it does not reproduce the near wall peak, as expected. The improvement brought about by the use of the damping function (13) is apparent on the dissipation profile, which is now in fair agreement with DNS data, opposite to the dissipation profile predicted by the BSL model which exhibits too strong a peak in the buffer layer and falls down at the wall.

The three diagonal stresses are plotted in figure 4. “BSL” values are obtained assuming $\overline{u'^2} = k$, $\overline{v'^2} = 0.4k$, $\overline{w'^2} = 0.6k$. $\overline{v'^2}$ profile is well reproduced, $\overline{w'^2}$ is depleted in the buffer region and $\overline{u'^2}$ and $\overline{w'^2}$ are underestimated, but not in the same region, $\overline{w'^2}$ being underestimated closer to the wall, while the near wall peak of $\overline{u'^2}$ is well reproduced but $\overline{u'^2}$ is underestimated further from the wall. Profiles of all turbulent quantities are very similar to the ones provided by the $k-\omega$ model in the logarithmic region and above.

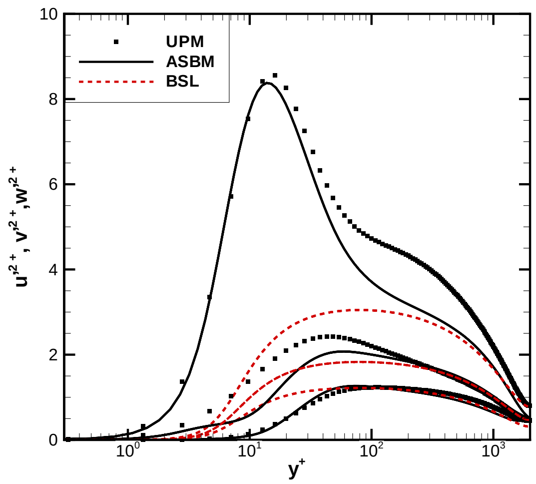

Figure 4: Channel flow $R_\tau = 2000$ – Diagonal stresses predictions

Couette–Poiseuille flows

In the framework of the WALLTURB program, DNS of Couette–Poiseuille flows were performed by the Roma University. Two Reynolds numbers, roughly corresponding to $R_\tau = 100$ and 200 and three lower wall velocities, giving Couette, intermediate and Poiseuille type flows, were considered (0rlandi, 2008).

Predicted velocity profiles for the six cases are compared to DNS in figure 5. From bottom to top, the profiles are shifted and correspond to Poiseuille, intermediate and Couette flow, the lowest curve being for the lowest Reynolds number. Some discrepancies can be noted for the Poiseuille type flow but the overall agreement is very good.

Reynolds stress profiles for the intermediate flow case, at the highest Reynolds number, are plotted in figure 6. In all

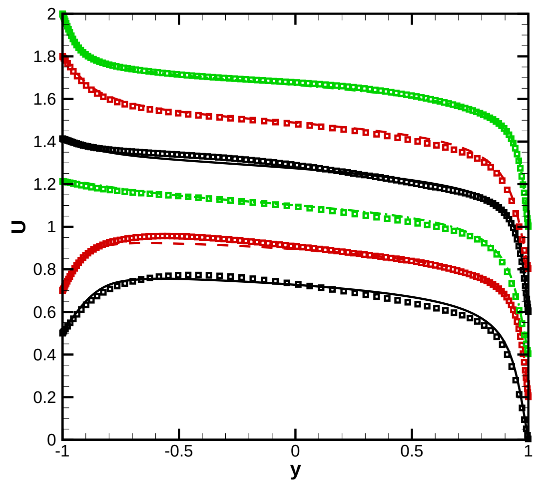

Figure 5: Predictions of the mean velocity profiles for the Couette–Poiseuille flows

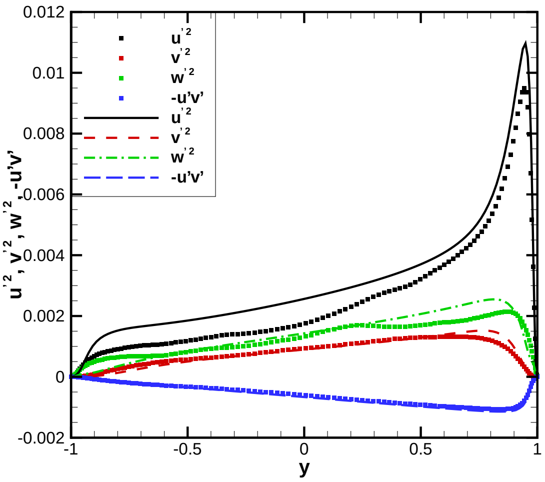

Figure 6: Reynolds stress predictions for the intermediate type flow

flow cases, the longitudinal component u'^2 is slightly overestimated but the overall agreement is fair. Comparisons have also been performed on the dimensionality and circulicity tensors which characterize the underlying turbulent structures. Some discrepancies are found at low Reynolds number, especially close to the moving wall, but the overall agreement is satisfactory.

Zero pressure gradient boundary layers

Skin friction coefficient predictions for zero pressure gradient boundary layers are compared with Fernholz' (1996) and Kármán-Schoennher correlations. After an initial transient, models relax to very low error levels, the present model being comparable to Spalart and SST ones.

Comparisons were also performed with experimental data for high Reynolds number boundary layers obtained in the framework of WALLTURB in Laboratoire de Mécanique de Lille (LML). Changing the flow velocity, boundary layer

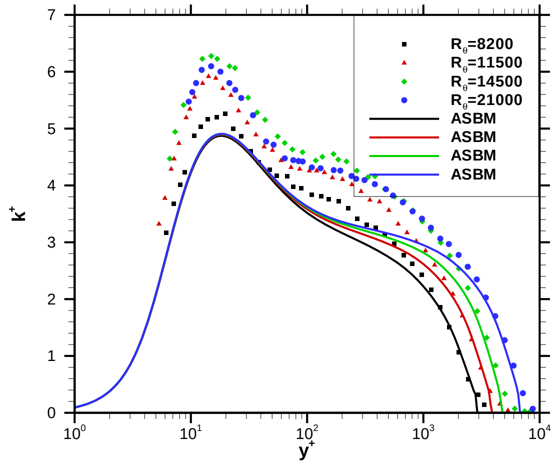

Figure 7: Zero pressure gradient boundary layers –Turbulent kinetic energy profile for various Reynolds numbers

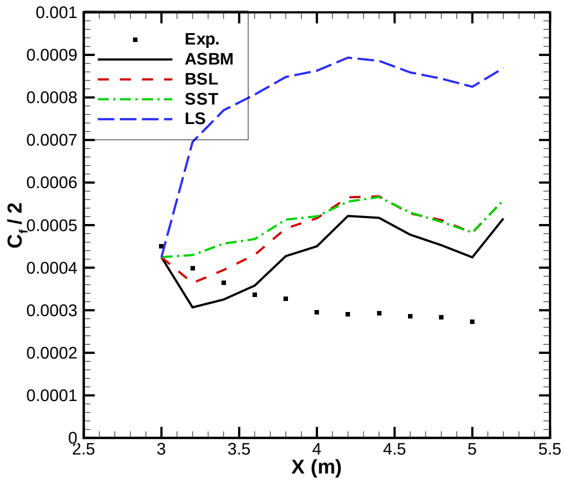

Figure 8: Skin friction predictions for Skåre and Krogstad strong adverse pressure gradient experiment

data for Reynolds number based upon the momentum thickness $R_\theta = 8200$, 11500, 14500 and 21000 have been obtained. Nice agreement is achieved for the mean velocity profiles. However, as shown in figure 7, the present model, as other standard models, yields the same solution for the non-dimensional turbulent kinetic energy profile in the wall region whatever the Reynolds number. This is logical when considering the way the wall treatment has been designed. $u^+(y^+)$ and hence $\frac{\partial u^+}{\partial y^+}$ and $-\overline{u'v'}^+$ are assumed universal, in agreement with DNS data. As there is nothing in the ASBM model to account for inactive motions, it also yields universal profiles for all the diagonal stresses and the turbulent kinetic energy, in contradiction with the Reynolds number dependence evidenced by de Graaf and Eaton (2000).

Adverse pressure gradient boundary layers

At last, several adverse pressure gradient test cases have been considered. Only the most difficult case, i.e. the nearly equilibrium flow subjected to a strong adverse pres-

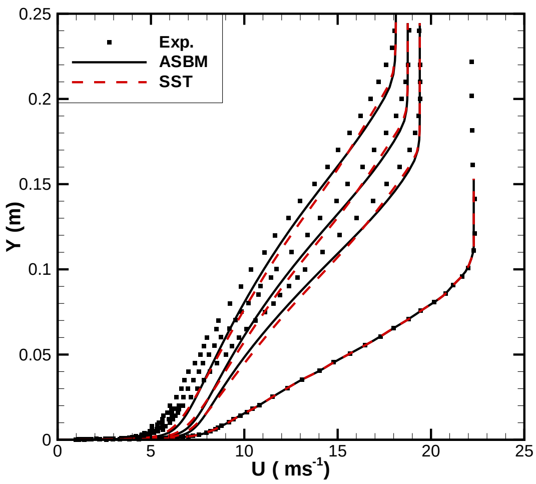

Figure 9: Mean velocity profile predictions for Skåre and Krogstad strong adverse pressure gradient experiment - From right to left stations X = 3. , 4.2 , 4.6 and 5m

sure gradient investigated by Skåre and Krogstad (1994) is presented. Figure 8 shows that the present model better predicts the low skin friction levels than the BSL model it is based upon, even when SST correction is applied. Launder and Sharma (1974) $k-\varepsilon$ model predictions are also plotted (LS) to evidence the improvement brought by the use of the ω equation.

Figure 9 compares velocity profile predictions at various stations, profiles moving from right to left when going downstream. The improvement brought by the present model w.r.t. the SST model is retrieved.

CONCLUSIONS AND PERSPECTIVES

An easy way to use the Algebraic Structure Based Model, coupling it with the widespread BSL model, has been proposed. It only requires slight modifications of the BSL part, besides of course adding an ASBM routine to compute the Reynolds stress tensor. A rationale to derive the wall correction has been proposed. The present model thus gives access to the much better representation of the Reynolds stress tensor, e.g. for flows with rotation, provided by the ASBM model.

The model has been tested on simple sheared flows such as Poiseuille, Couette-Poiseuille and boundary layer flows, for which it gave fair predictions and rather nicely reproduced the near wall turbulence, what the basic BSL model is not able of. Improvements to represent "inactive motions" have to be considered. The information about the turbulent structures available in the ASBM model could be used to improve the ω equation, as in Reynolds et al. (2002).

Author names appear in alphabetical order.

This work has been performed under the WALLTURB project. WALLTURB (A European synergy for the assessment of wall turbulence) is funded by the EC under the 6th framework program (CONTRACT N: AST4-CT-2005-516008)

REFERENCES

Aupoix B., Kassinos S.C., and Langer C.A. ASBM-BSL: An easy access to the Structure Based Model technology. In M. Stanislas, editor, *Progress in Wall Turbulence: Understanding and Modelling*, Lille, France, April, 21-23 2009. WallTurb, Springer.

de Graaf D.B. and Eaton J.K. Reynolds number scaling of the flat-plate turbulent boundary layer. *Journal of Fluid Mechanics*, 422:319–346, 2000.

Fernholz H.H. and Finley P.J. The incompressible zero-pressure gradient turbulent boundary layer: An assessment of the data. *Progress in Aerospace Sciences*, 32:245–311, 1996.

Haase W., Aupoix B., Bunge U., and Schwamborn D., editors. *FLOMANIA – A European Initiative on Flow Physics Modelling*, volume 94 of *Notes on Numerical Fluid Mechanics and Multidisciplinary Design.* Springer, 2006.

Hoyas S. and Jimenez J. Scaling of velocity fluctuations in turbulent channels up to $Re_\tau = 2000$. *Physics of Fluids*, 18:011702, 2006.

Kassinos S.C., Langer C.A., Haire S.L., and Reynolds W.C. Structure-based turbulence modelling for wall bounded flows. *International Journal of Heat and Fluid Flows*, 21:599–605, 2000.

Kassinos S.C., Reynolds W.C. , and Rogers M.M. One-point turbulence structure tensors. *Journal of Fluid Mechanics*, 428:213–248, 2001.

Launder B.E. and Sharma B.I. Application of energy-dissipation model of turbulence to the calculation of flow near a spinning disc. *Letters in Heat and Mass Transfer*, 1:131-138, 1974.

Menter F.R. Influence of freestream values on $k-\omega$ turbulence model predictions. *AIAA Journal*, 30(6):1657–1659, June 1992.

Peng S.H., Davidson L., and Holmberg S. A modified low-Reynolds number $k-\omega$ model for recirculating flows. *Journal of Fluid Engineering*, 119:867–875, December 1997.

Orlandi P. Database of turbulent channel flow with moving walls. http://dma.ing.uniroma1.it/users/orlandi/, 2008.

Reynolds W.C., Kassinos S.C., Langer C.A., and Haire S.L. New directions in turbulence modeling. In *Third International Symposium on Turbulence, Heat and Mass Transfer*, Nagoya, Japan, April 3-6 2000.

Reynolds W.C., Langer C.A., and Kassinos S.C. Structure and scales in turbulence modelling. *Physics of Fluids*, 14(7):2485–2492, 2002.

Skåre P.E. and Krogstad P-Å. A turbulent equilibrium boundary layer near separation. *Journal of Fluid Mechanics*, 272:319–348, August 1994.

Skote M., Henningson D.S., and Henkes R.A.W.M. Direct numerical simulation of self-similar turbulent boundary layers in adverse pressure gradients. *Flow, Turbulence and Combustion*, 60:47–85, 1998.

Spalart P.R. Direct simulation of a turbulent boundary layer up to $R_\theta = 1410$. *Journal of Fluid Mechanics*, 187:61–98, 1988.

Spalart P.R. and Allmaras S.R. A one-equation turbulence model for aerodynamic flows. *La Recherche Aérospatiale*, 1:5–21, 1994.

Wilcox D.C. Reassessment of the scale-determining equation for advanced turbulence models. *AIAA Journal*, 26(11):1299–1310, November 1988.

Wilcox D.C. Comparison of two-equation turbulence models for boundary layers with pressure gradients. *AIAA Journal*, 31(8):1414–1421, August 1993.